

U.S. Woce Indian Ocean Survey: Final Report for Radiocarbon

Robert M. Key and Paul D. Quay

July 12, 2002

1.0 General Information

The U.S. WOCE Indian Ocean Survey consisted of 9 cruises covering the period December 1, 1994 to January 22, 1996. All of the cruises used the R/V Knorr operated by the Woods Hole Oceanographic Institute. A total of 1244 hydrographic stations were occupied with radiocarbon sampling on 366 stations. The radiocarbon stations are shown as black dots in Figure 1. To give an indication of the total radiocarbon coverage for the Indian Ocean, the figure includes radiocarbon stations from WOCE sections S4I (Key, 1999; red dots) and I6S (Leboucher, *et al.*, 1999; white dots) and from the earlier GEOSECS (Stuiver and Ostlund, 1983; brown dots) and INDIGO (Bard, *et al.*, 1988; yellow dots) expeditions. Specific summary information on the 9

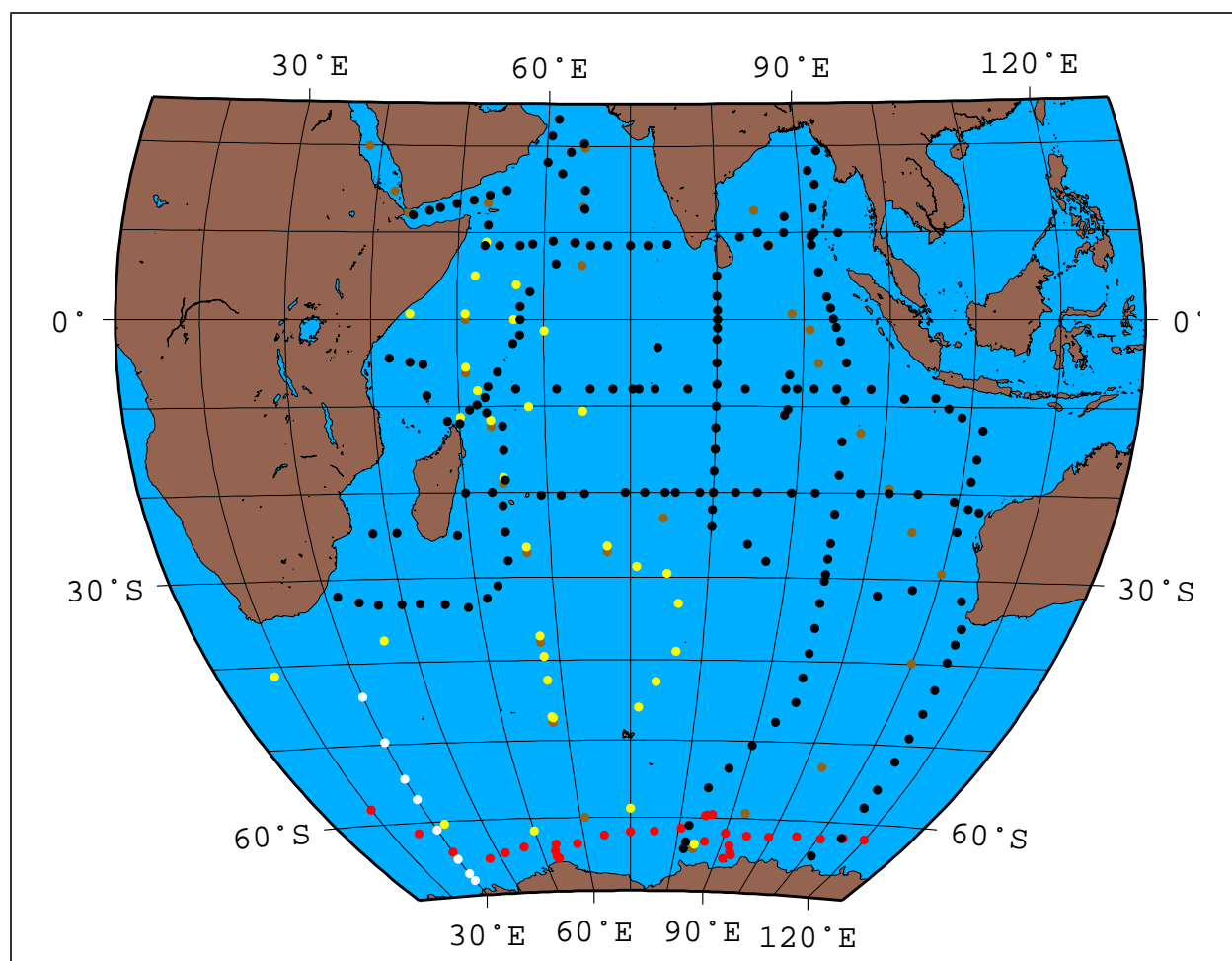


Figure 1: AMS ¹⁴C station map for WOCE S4I.

WOCE survey cruises is given in Table 1.

TABLE 1. Summary for Survey Sections

| Cruise | Chief Scientist | Start | End | $\Delta^{14}\text{C}$ Stations | $\Delta^{14}\text{C}$ Samples |
|--------|-------------------------------------|-------------------------------------|-------------------------------------|--------------------------------|-------------------------------|
| I8SI9S | M. McCartney T. Whitworth | 12/01/94 Fremantle Australia | 01/19/95 Fremantle Australia | 26 | 662 |
| I9N | A. Gordon D. Olson | 01/24/95 Fremantle Australia | 03/05/95 Colombo Sri Lanka | 22 | 364 |
| I8NI5E | L. Talley M. Baringer | 03/10/95 Colombo Sri Lanka | 04/15/95 Fremantle Australia | 20 | 414 |
| I3 | W. Nowlin B. Warren | 04/20/95 Fremantle Australia | 06/07/95 Port Louis Mauritius | 20 | 462 |
| I5WI4 | J. Toole | 06/11/95 Port Louis Mauritius | 07/11/95 Port Louis Mauritius | 15 | 361 |
| I7N | D. Olson S. Doney D. Musgrave | 07/15/95 Port Louis Mauritius | 08/24/95 Muscat Oman | 22 | 373 |
| I1 | J. Morrison H. Bryden | 08/29/95 Muscat Oman | 10/16/95 Singapore | 24 | 426 |
| I10 | N. Bray J. Toole | 11/11/95 Dampier Australia | 11/28/95 Singapore | 6 | 127 |
| I2 | G. Johnson B. Warren | 12/02/95 Singapore China | 01/22/96 Mombasa Kenya | 28 | 651 |

2.0 Personnel

$\Delta^{14}\text{C}$ sampling for cruise I8SI9S was carried out by Melinda Brockington (University of Washington). Personnel for the remainder of the cruises came from the Ocean Tracer Lab (OTL Princeton University) and included G. McDonald, A. Doerty, R. Key, T. Key, and R. Rotter. $\Delta^{14}\text{C}$ (and accompanying $\delta^{13}\text{C}$) analyses were performed at the National Ocean Sciences AMS Facility (NOSAMS) at Woods Hole Oceanographic Institution. R. Key collected the data from NOSAMS, merged the files with hydrographic data, assigned quality control flags to the $\Delta^{14}\text{C}$ and submitted the results to the WOCE office (4/02). R. Key is P.I. for the ^{14}C data. P. Quay (U.W.) and A. McNichol (WHOI/NOSAMS) are P.I.s for the ^{13}C data. In addition to collecting samples the ship-board ^{14}C person was also responsible for operation of the underway pCO_2 system provided by the OTL (Sabine and Key, 1997; Sabine, *et al.*, 2000).

3.0 Results

This $\Delta^{14}\text{C}$ data set and any changes or additions supersedes any prior release.

3.1 Hydrography

Hydrographic data from these cruises were submitted to the WOCE office by the chief scientists and are described in various reports which are available from the web site (http://whpo.ucsd.edu/data/tables/onetime/1tim_ind.htm).

3.2 $\Delta^{14}\text{C}$

The $\Delta^{14}\text{C}$ values described here were originally distributed in the NOSAMS data reports listed in Table 2 and given in full in the References . Those reports included results which had not been through the WOCE quality control procedures. For WOCE applications, this report supersedes the NOSAMS reports.

TABLE 2. NOSAMS Data Report Summary

| Cruise | Report |
|-------------|--------|
| I8SI9S | 99-089 |
| I7N I9N | 99-144 |
| I1 | 99-199 |
| I8N | 00-218 |
| I3 I5W14 | 01-013 |
| I2 | 02-001 |

All of the AMS samples from these cruise have been measured using the AMS methods outlined in Key *et al.*, 1996 and citations therein (especially McNichol *et al.*, 1994; Osborne *et al.* 1994; and Scheideret *al.* 1995). Table 3 summarizes the number of samples analyzed and the quality control flags assigned for each cruise. Approximately 98% of the samples collected were deemed to be “good” (flagged 2 or 6). Quality flag values were assigned to all $\Delta^{14}\text{C}$ measurements using the code defined in Table 0.2 of WHP Office Report WHPO 91-1 Rev. 2 section 4.5.2. (Joyce, *et al.*, 1994). No measured values have been removed from this data set.

TABLE 3. Sample Analysis and QC Summary

| Cruise | Samples Analyzed | QC Flag Totals | | | | |
|--------|------------------|----------------|----|----|----|----|
| | | 2 | 3 | 4 | 5 | 6 |
| I8SI9S | 662 | 636 | 6 | 8 | 0 | 12 |
| I9N | 368 | 354 | 4 | 3 | 4 | 3 |
| I8NI5E | 416 | 401 | 6 | 0 | 2 | 7 |
| I3 | 463 | 448 | 5 | 0 | 1 | 9 |
| I5W14 | 366 | 342 | 3 | 1 | 5 | 15 |
| I7N | 383 | 370 | 3 | 0 | 10 | 0 |
| I1 | 430 | 421 | 2 | 2 | 4 | 1 |
| I10 | 127 | 127 | 0 | 0 | 0 | 0 |
| I2 | 655 | 636 | 13 | 2 | 4 | 0 |
| Total | 3870 | 3735 | 42 | 16 | 30 | 47 |

4.0 Data Summary

Figures 2-6 summarize the $\Delta^{14}\text{C}$ data collected during the Indian Ocean survey. Only $\Delta^{14}\text{C}$ measurements with a quality flag value of 2 (“good”) or 6 (“replicate”) are included in the figures. Figure 2 shows the $\Delta^{14}\text{C}$ values with 2σ error bars plotted as a function of pressure. The

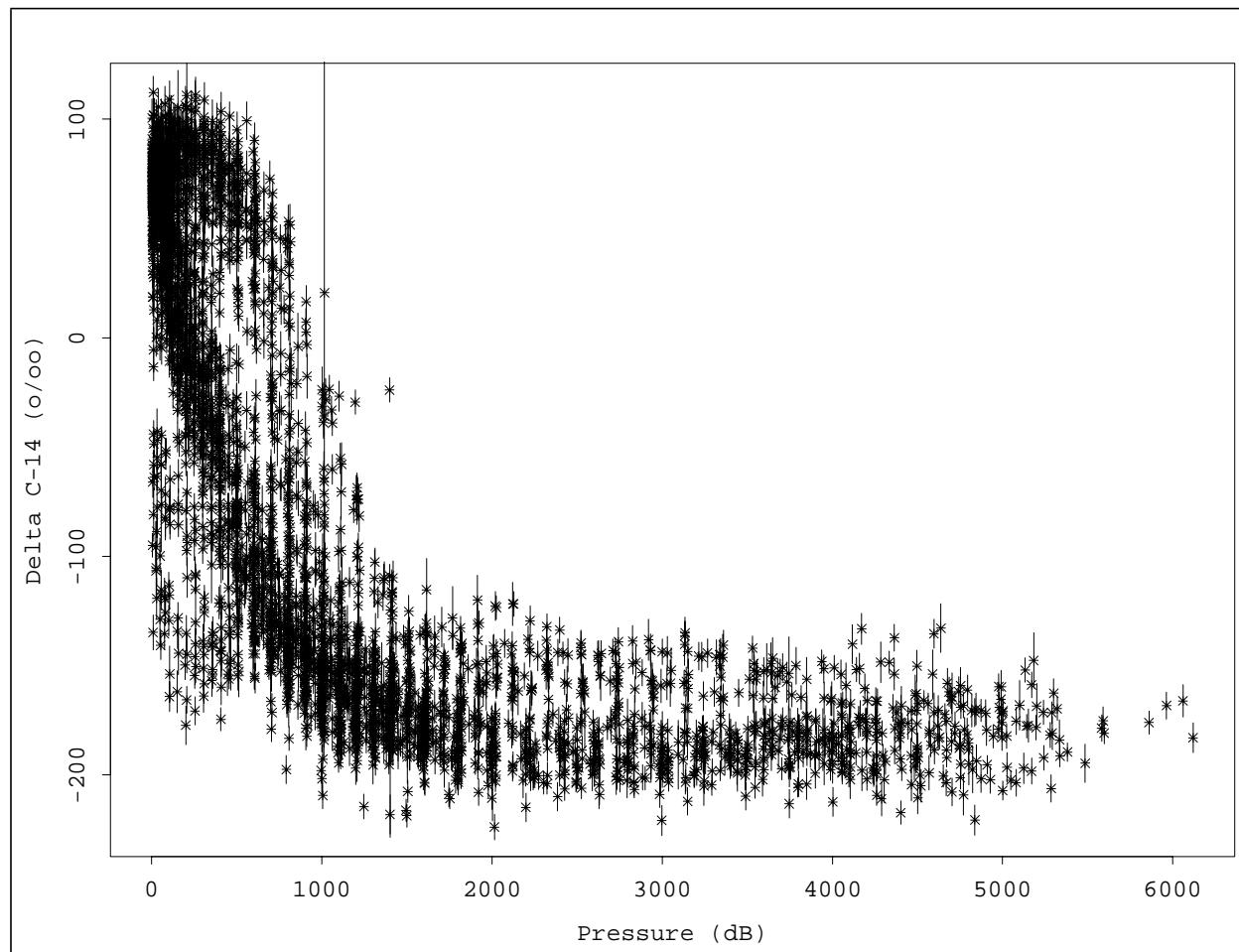


Figure 2: $\Delta^{14}\text{C}$ results shown with 2σ error bars.

mid depth $\Delta^{14}\text{C}$ minimum which occurs around 2500 meters in the Pacific is not apparent in these data. In fact, there is very little variation in the deep and bottom water other than the previously reported decrease in $\Delta^{14}\text{C}$ from south to north. All of the samples collected at a depth greater than 1000 meters have a mean $\Delta^{14}\text{C} = -165 \pm 25\text{‰}$ (standard error = 0.5‰ with $n=2086$). A substantial fraction of this variability is due to the difference between the Southern Ocean and main basin deep waters.

Figure 3 shows the deep ($>1000\text{m}$) $\Delta^{14}\text{C}$ values plotted against silicate. The black and red points are from north and south of 35°S , respectively. The straight line shown in the figure is the least squares regression relationship derived by Broecker *et al.* (1995) based on the GEOSECS global data set. According to their analysis, this line ($\Delta^{14}\text{C} = -70 - \text{Si}$) represents the relationship between naturally occurring radiocarbon and silicate for most of the ocean. They noted that the technique could not be simply applied at high latitudes as confirmed by this data set.

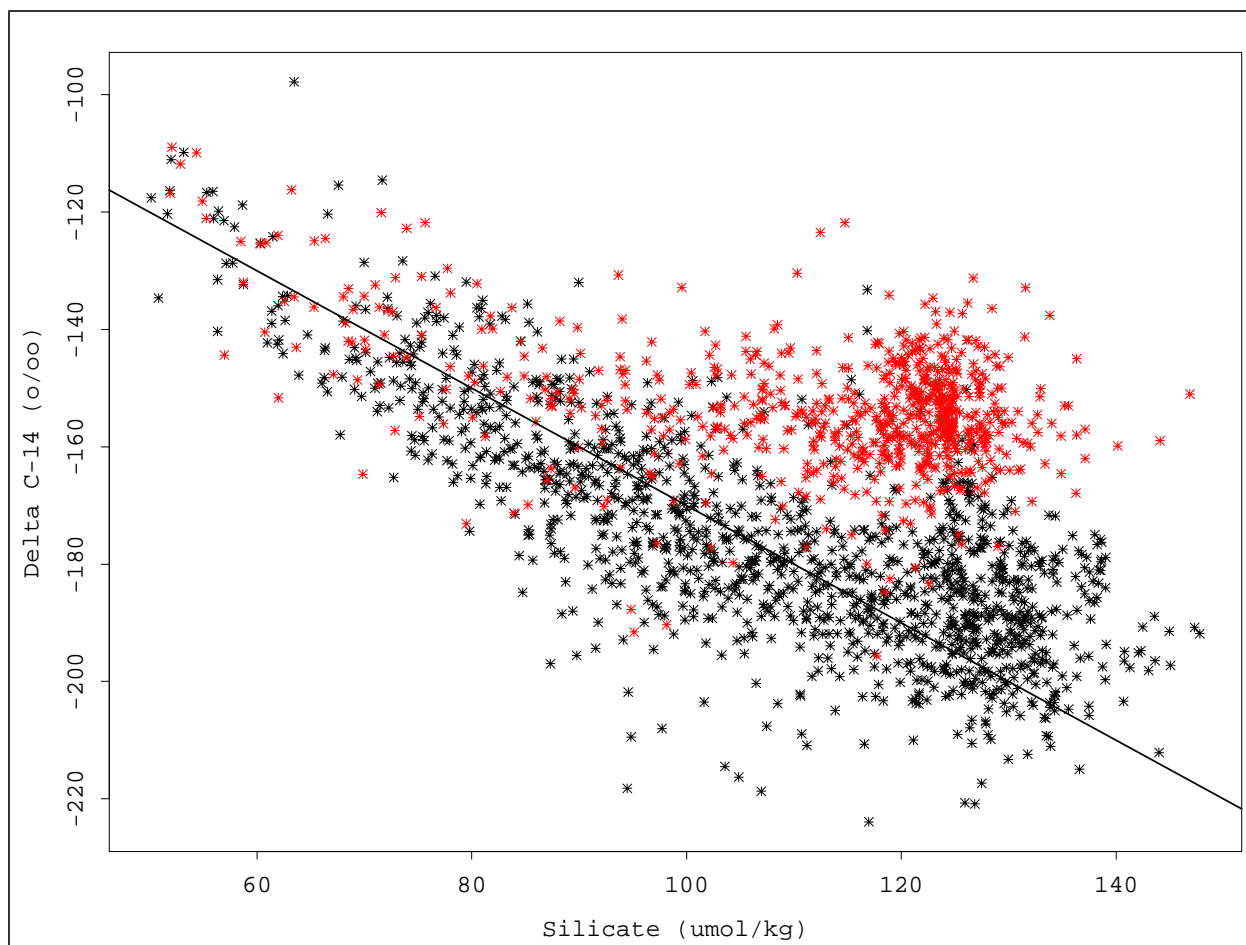


Figure 3: $\Delta^{14}\text{C}$ as a function of silicate for samples collected deeper than 1000m. The black points are from north of 35°S and the red points south of 35°S . The straight line shows the relationship proposed by Broecker, *et al.*, 1995 ($\Delta^{14}\text{C} = -70 - \text{Si}$ with radiocarbon in ‰ and silicate in $\mu\text{mol/kg}$).

Figure 4 shows all of the radiocarbon values plotted against potential alkalinity (defined as $[\text{alkalinity} + \text{nitrate}] * 35 / \text{salinity}$). The straight line is the regression fit ($^{14}\text{C} = -59 - 0.962(\text{PALK} - 2320)$) derived by Rubin and Key (2002) using GEOSECS measurements assumed to have no bomb-produced $\Delta^{14}\text{C}$. The value 2320 is the estimated surface ocean mean potential alkalinity. As with Figure 3 the black and red points in Figure 4 indicate measurements taken north and south of 35°S , respectively. Unlike the silicate plot (Figure 3), there is no apparent difference in the relationship for Southern Ocean vs Indian Ocean deep waters. The distance a point falls above the regression line is an estimate of the bomb radiocarbon contamination for the sample.

Figures 5-9 show gridded sections of the $\Delta^{14}\text{C}$ data. In each figure the water column is divided into upper (0-1000m) and lower (1000-bottom) portions. The data were gridded using the loess method (Chambers *et al.*, 1983; Chambers and Hastie, 1991; Cleveland, 1979; Cleveland and Devlin, 1988). The span for the fits was adjusted to be minimum and yet capture the large scale features. The contour interval is 10‰ for the upper water column and 20‰ for intermediate and deep water.

Figure 5 and Figure 6 show the meridional $\Delta^{14}\text{C}$ distribution in the eastern and western Indian Ocean. In both figures the distribution pattern is very similar to that seen in the Pacific

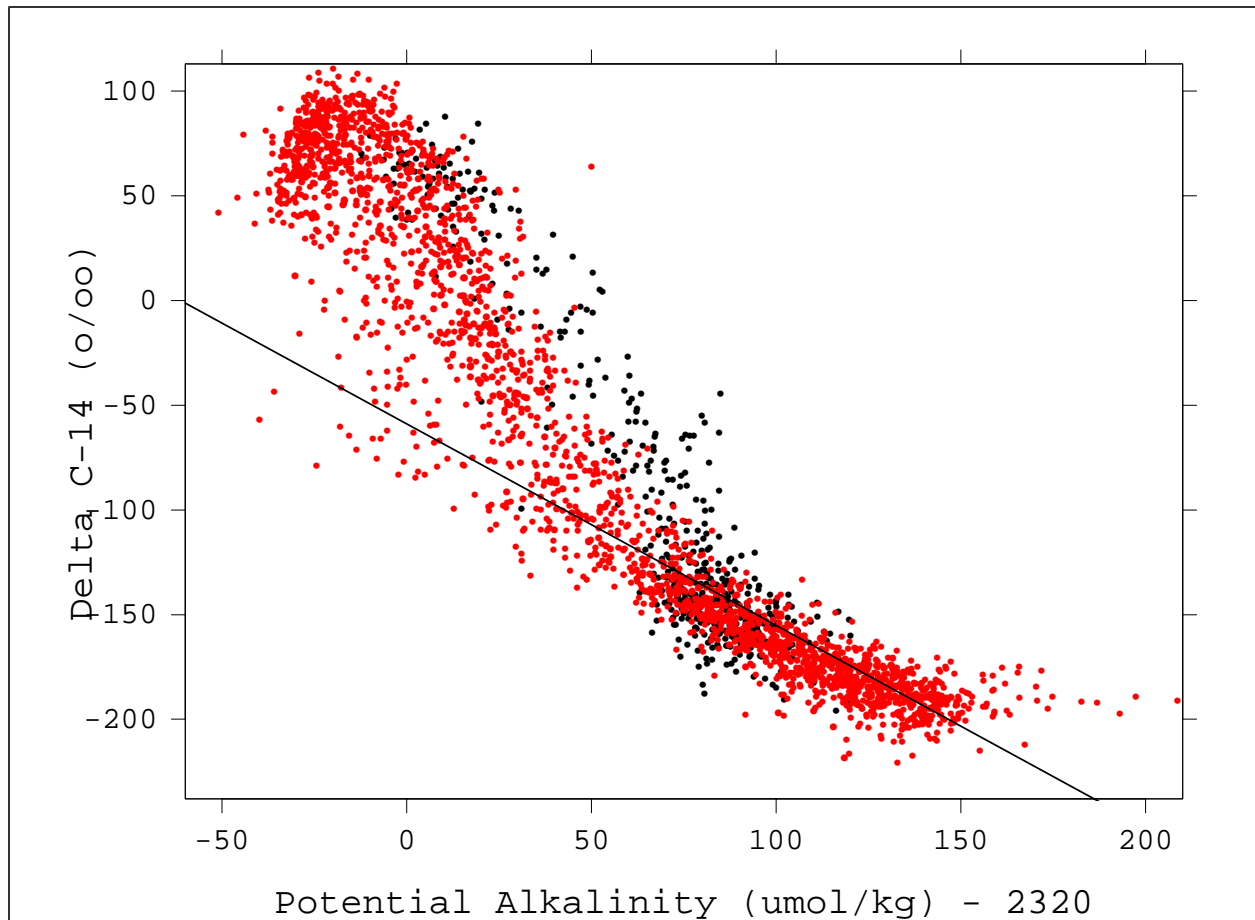


Figure 4: Based on the potential alkalinity method (Rubin and Key, 2002), the samples which plot above the line and have potential alkalinity values less than about 2400 $\mu\text{mole/kg}$ are contaminated with bomb-produced ^{14}C .

Ocean WOCE samples. In the Pacific the maximum $\Delta^{14}\text{C}$ values were frequently found in shallow water, but beneath the surface. In the Indian Ocean data a subsurface maximum is not so common. Both sections show intrusion of Circumpolar Deep Water from the south along the bottom and return flow of deep water at 2000-3000m. As with the Pacific the middepth waters have the lowest $\Delta^{14}\text{C}$ values, however the middepth Indian Ocean waters have significantly higher values than corresponding Pacific waters. This pattern is consistent with a mean ageing of waters from the Atlantic to Indian to Pacific.

Figure 7, Figure 8 and Figure 9 show zonal $\Delta^{14}\text{C}$ sections along the WOCE lines I1 ($\sim 10^\circ\text{N}$), I2 ($\sim 8^\circ\text{S}$) and I3 ($\sim 20^\circ\text{S}$). Except for the western ends, the $\Delta^{14}\text{C}$ contours in the upper kilometer are relatively flat. In each section the deep waters of the western basins have somewhat higher $\Delta^{14}\text{C}$ than at the same depth in the eastern basins. The strength of this signal decreases from south to north and is almost certainly due to the western basins having a higher fraction of North Atlantic Deep Water.

Figure 10 shows the meridional distribution of bomb produced $\Delta^{14}\text{C}$ (via Rubin and Key, 2002) in the eastern and western Indian Ocean. The eastern section used all WOCE samples collected at depths less than 1000m and east of 85°E . The western section uses the same depth range, but samples from west of 75°E . Both sections are contoured and colored in potential density space rather than against depth. One might expect *a priori* that the distributions would differ north of the

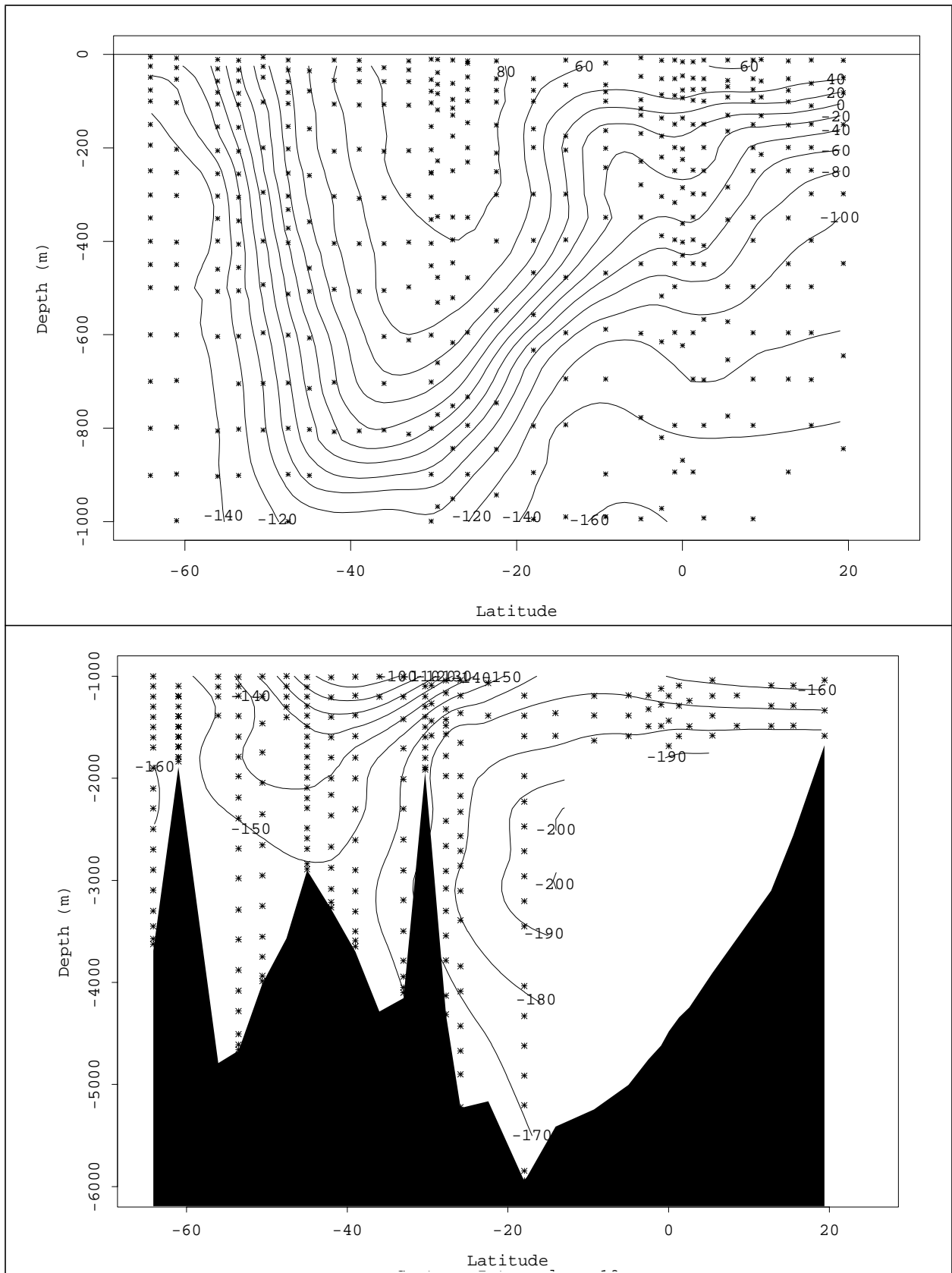


Figure 5: $\Delta^{14}\text{C}$, along I8S and I9N in the eastern Indian Ocean.

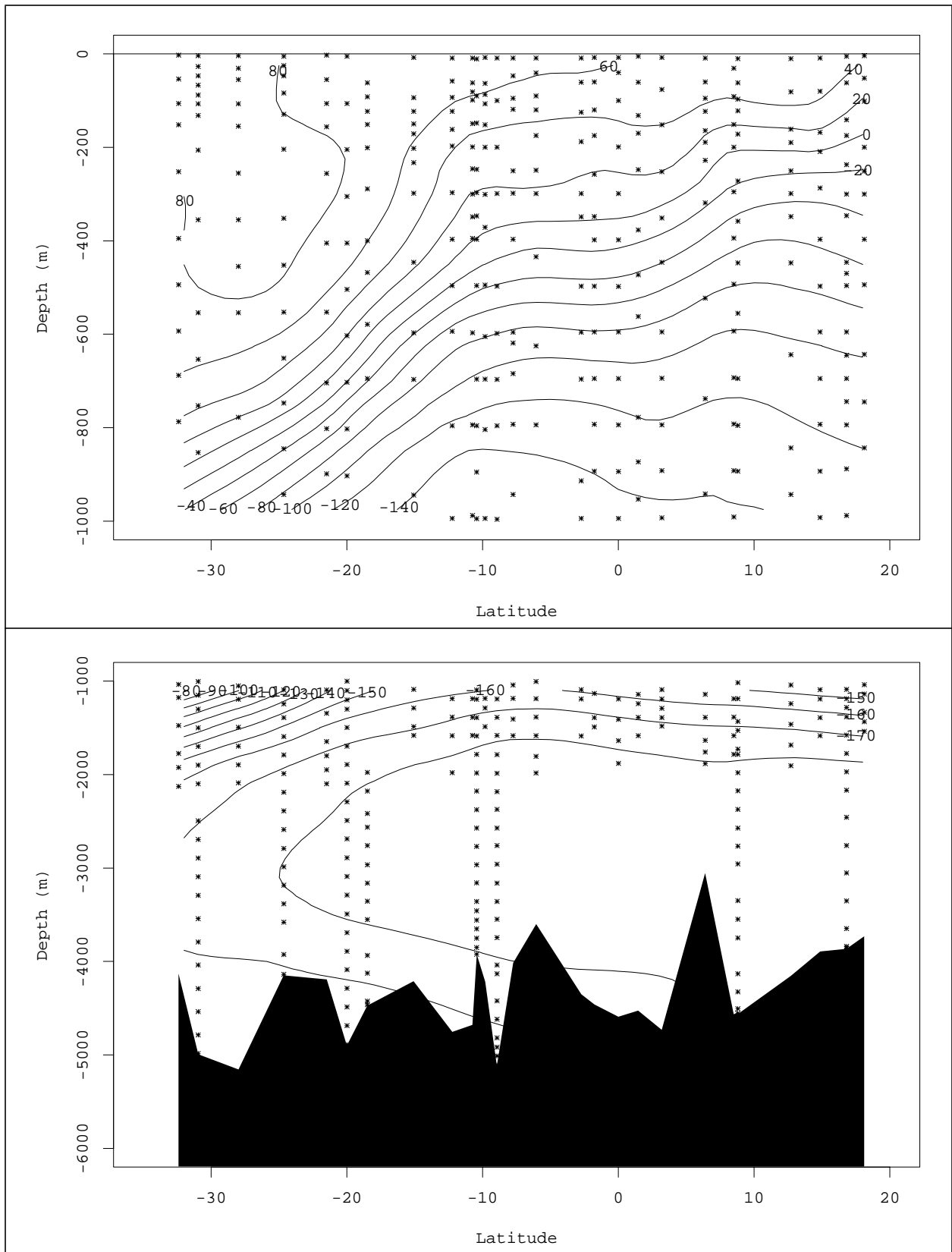


Figure 6: $\Delta^{14}\text{C}$ along I7 in the western Indian Ocean.

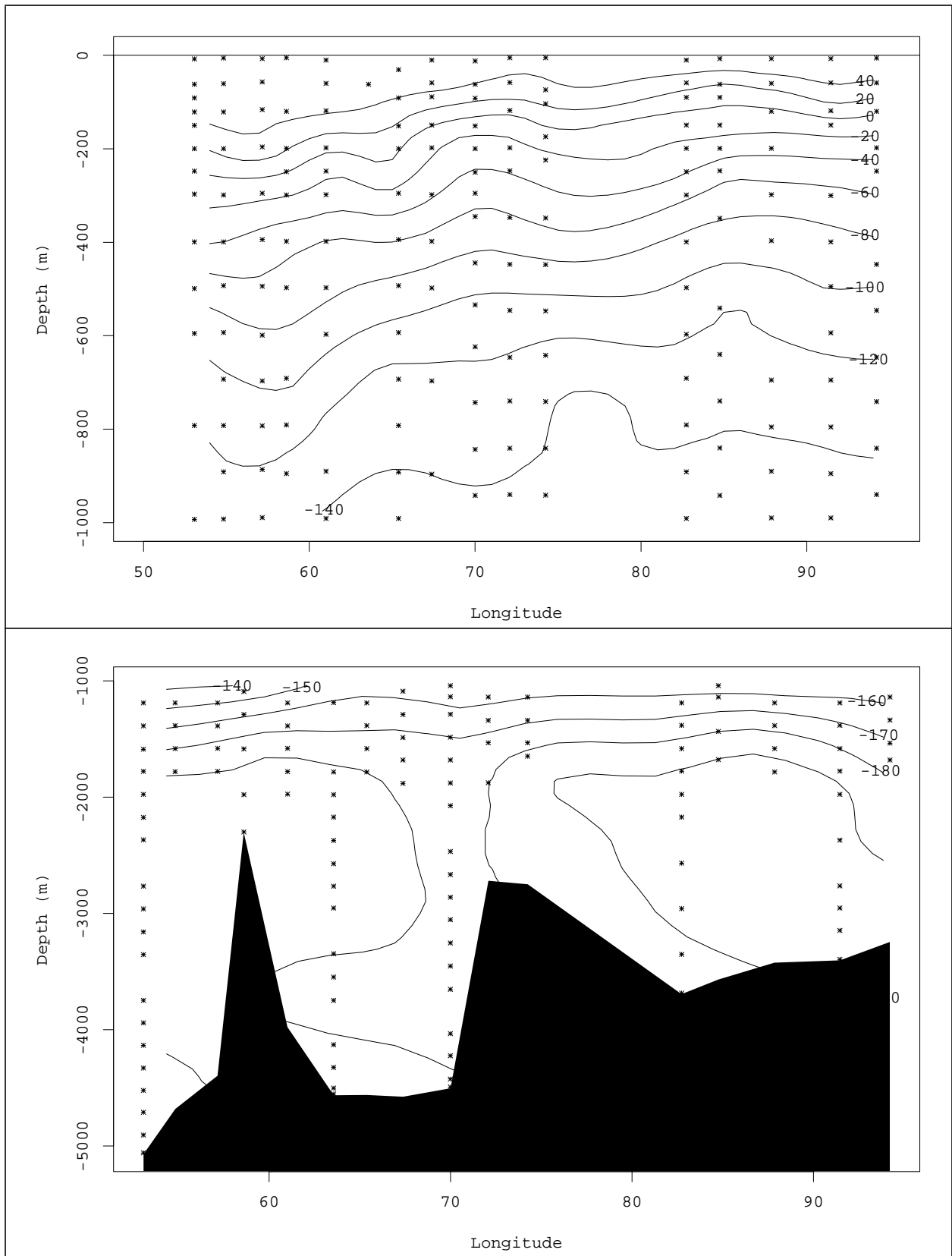


Figure 7: $\Delta^{14}\text{C}$ along I1 in the northern Indian Ocean.

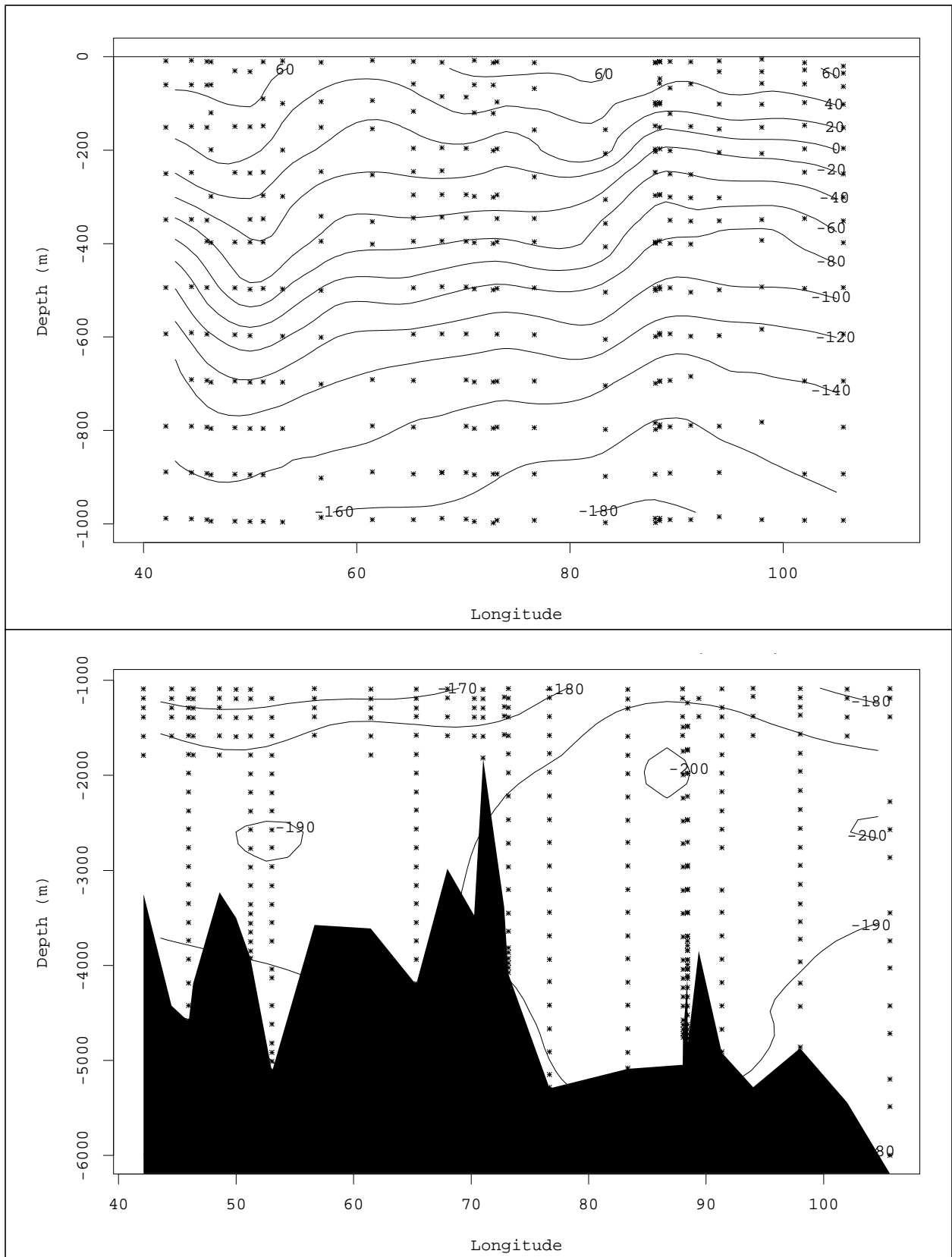


Figure 8: $\Delta^{14}\text{C}$ along I2 in the southern tropical Indian Ocean.

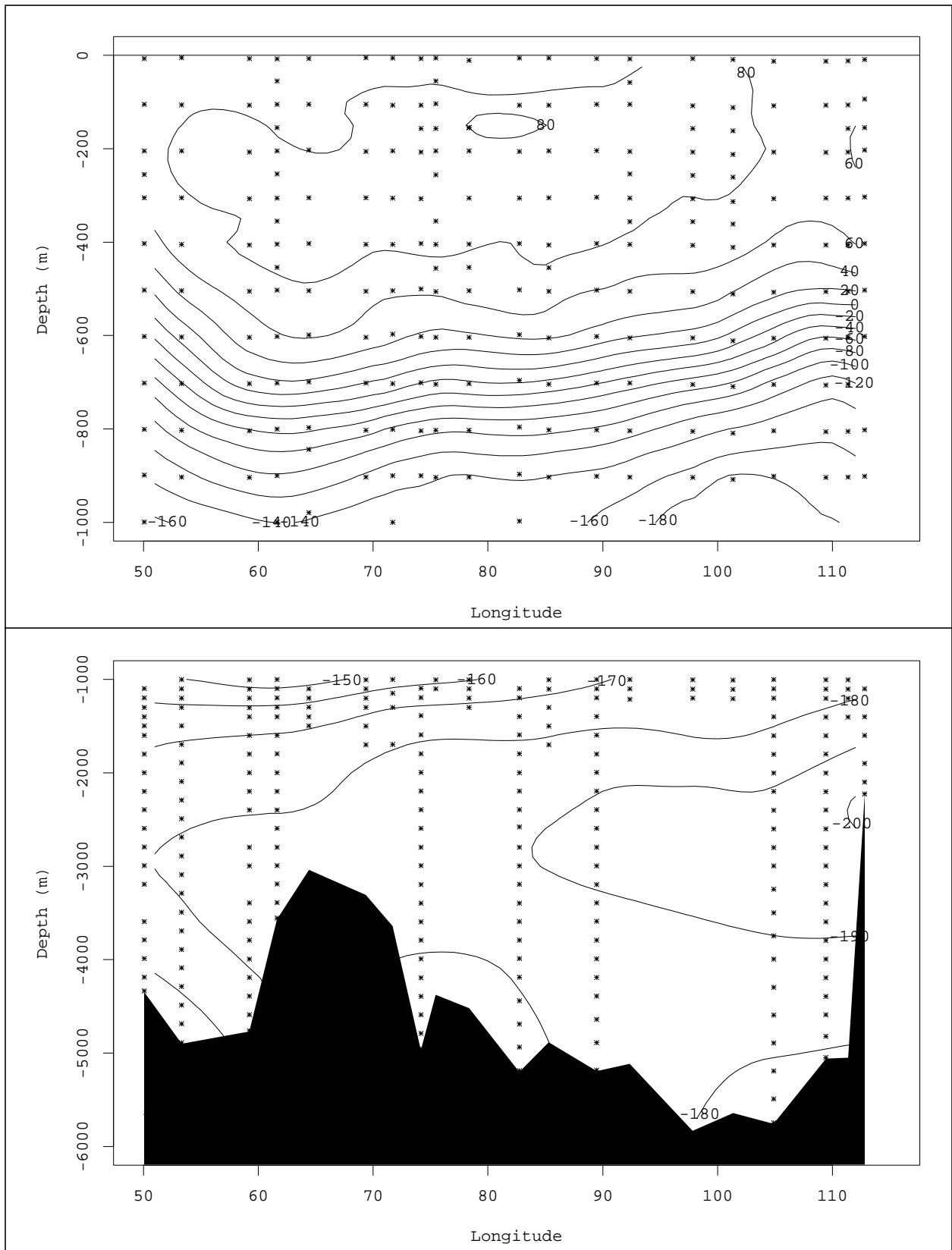


Figure 9: $\Delta^{14}\text{C}$ along I3 in the southern subtropical Indian Ocean at approximately 20°S.

equator due to the geography and difference in chemistry between the Bay of Bengal and Arabian Sea. Perhaps unexpected is the fact that the distributions differ significantly as far as 40°S. In the eastern section the maximum bomb $\Delta^{14}\text{C}$ values are found between 40°S and 20°S and more or less uniformly from the surface down to the level where $\sigma_\theta \sim 26.5$. The western section has a maximum in the same latitude range but in this case the maximum occurs as a subsurface lens.

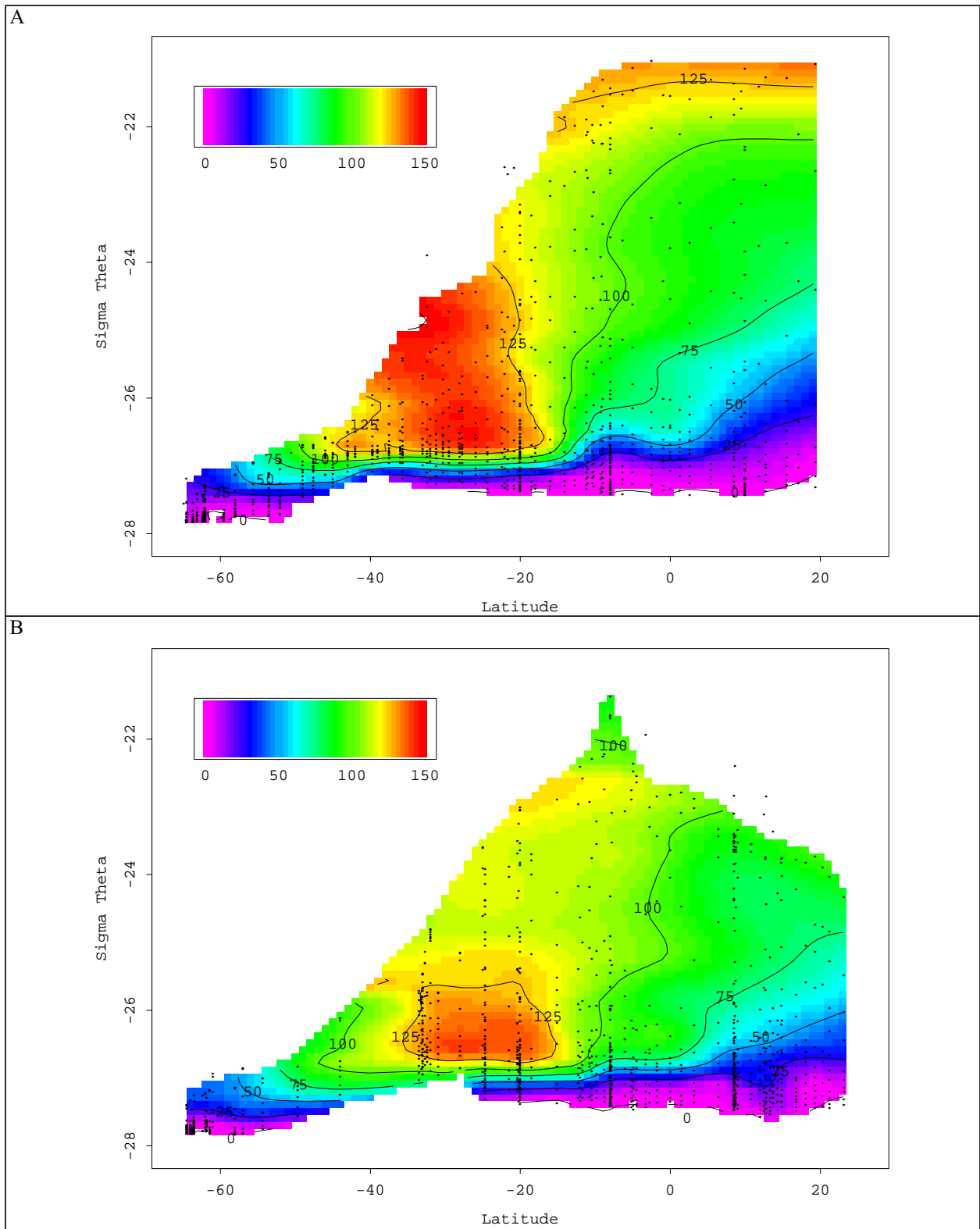


Figure 10: Mean bomb-produced $\Delta^{14}\text{C}$ sections in the eastern (A) and western (B) Indian Ocean, shown in potential density space for samples from the upper 1000m.

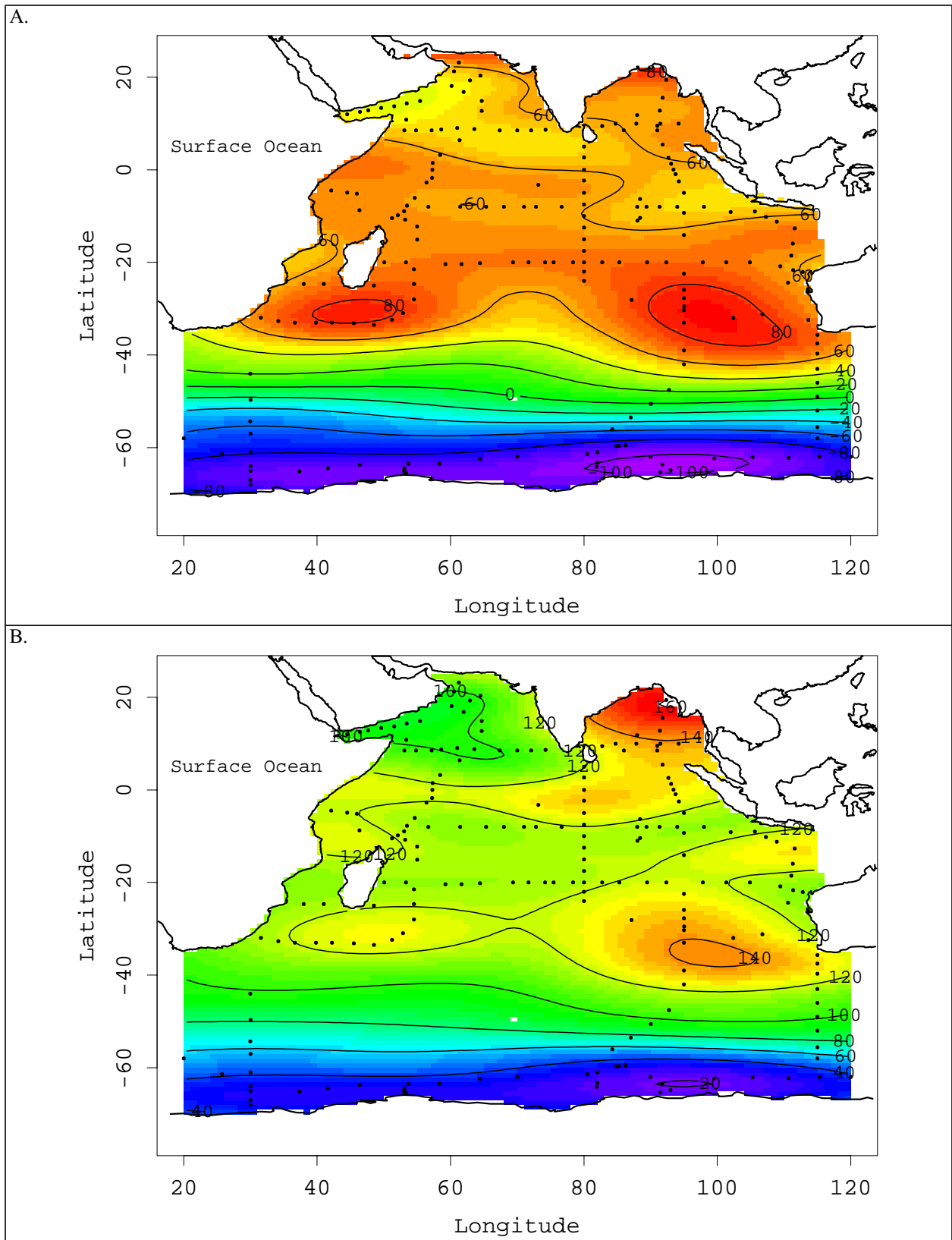


Figure 11: (A) $\Delta^{14}\text{C}$ and (B) bomb-produced $\Delta^{14}\text{C}$ for the surface Indian Ocean from WOCE measurements.

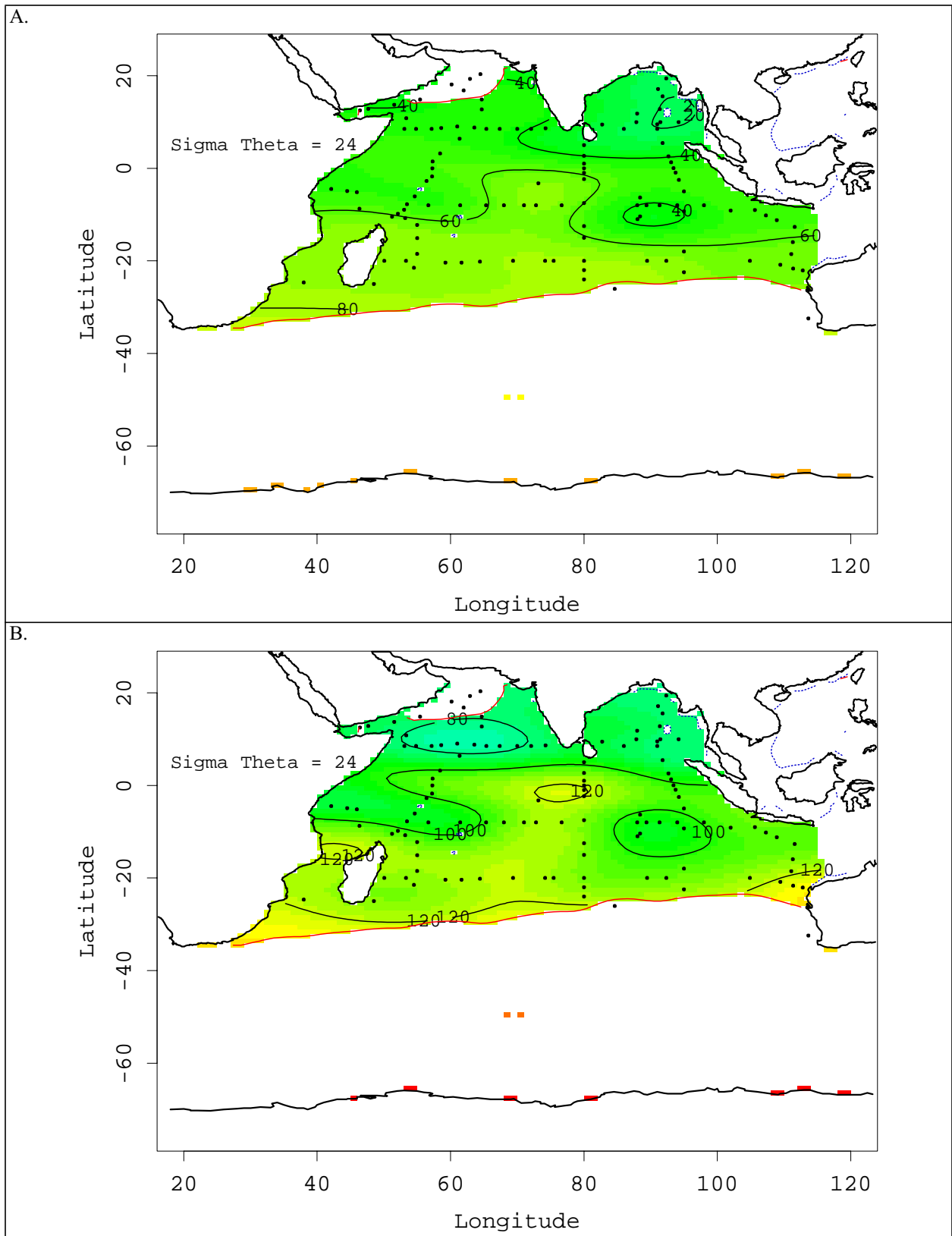


Figure 12: (A) $\Delta^{14}\text{C}$ and (B) bomb-produced $\Delta^{14}\text{C}$ on $\sigma_{\theta}=24.0$.

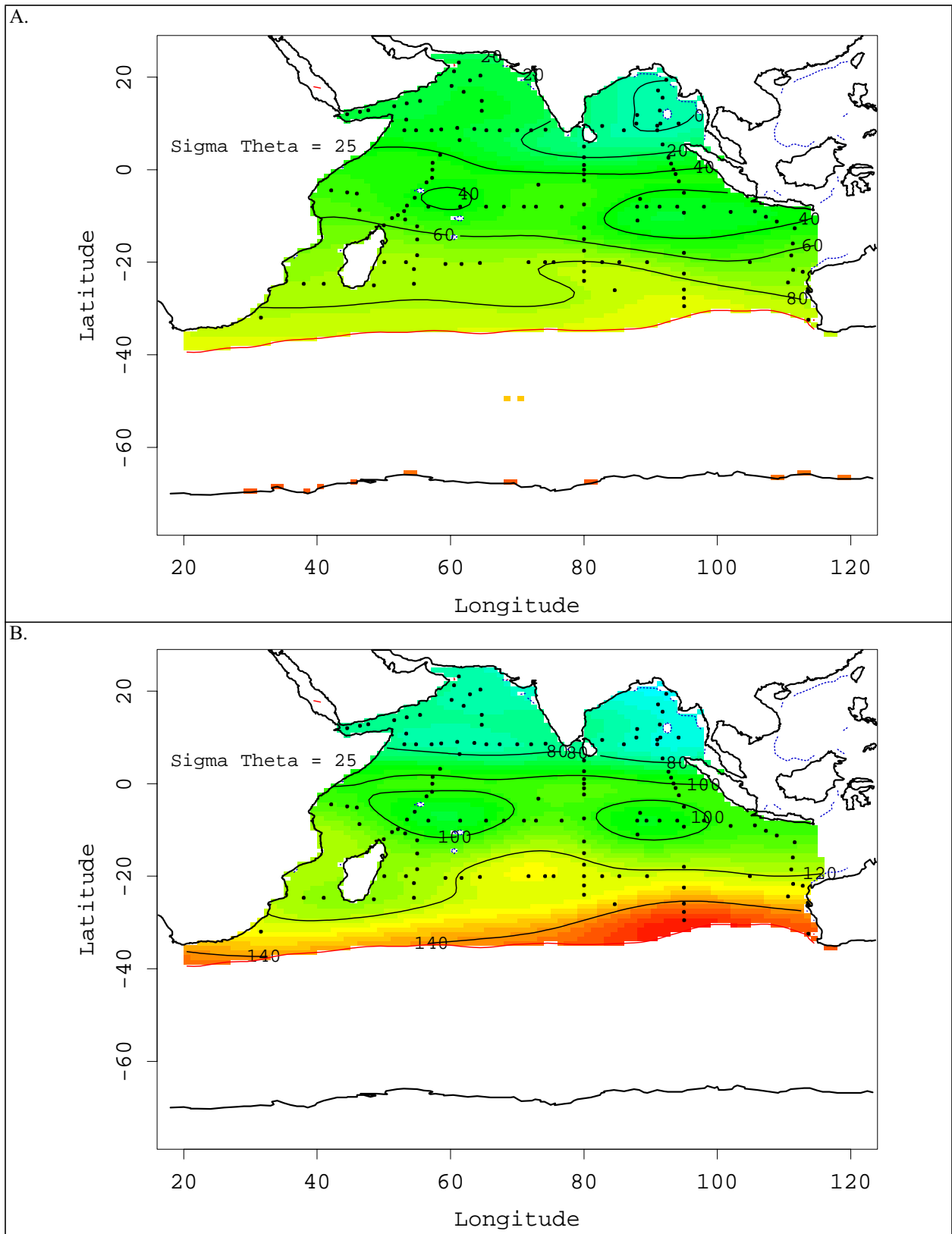


Figure 13: (A) $\Delta^{14}\text{C}$ and (B) bomb-produced $\Delta^{14}\text{C}$ on $\sigma_\theta=25.0$

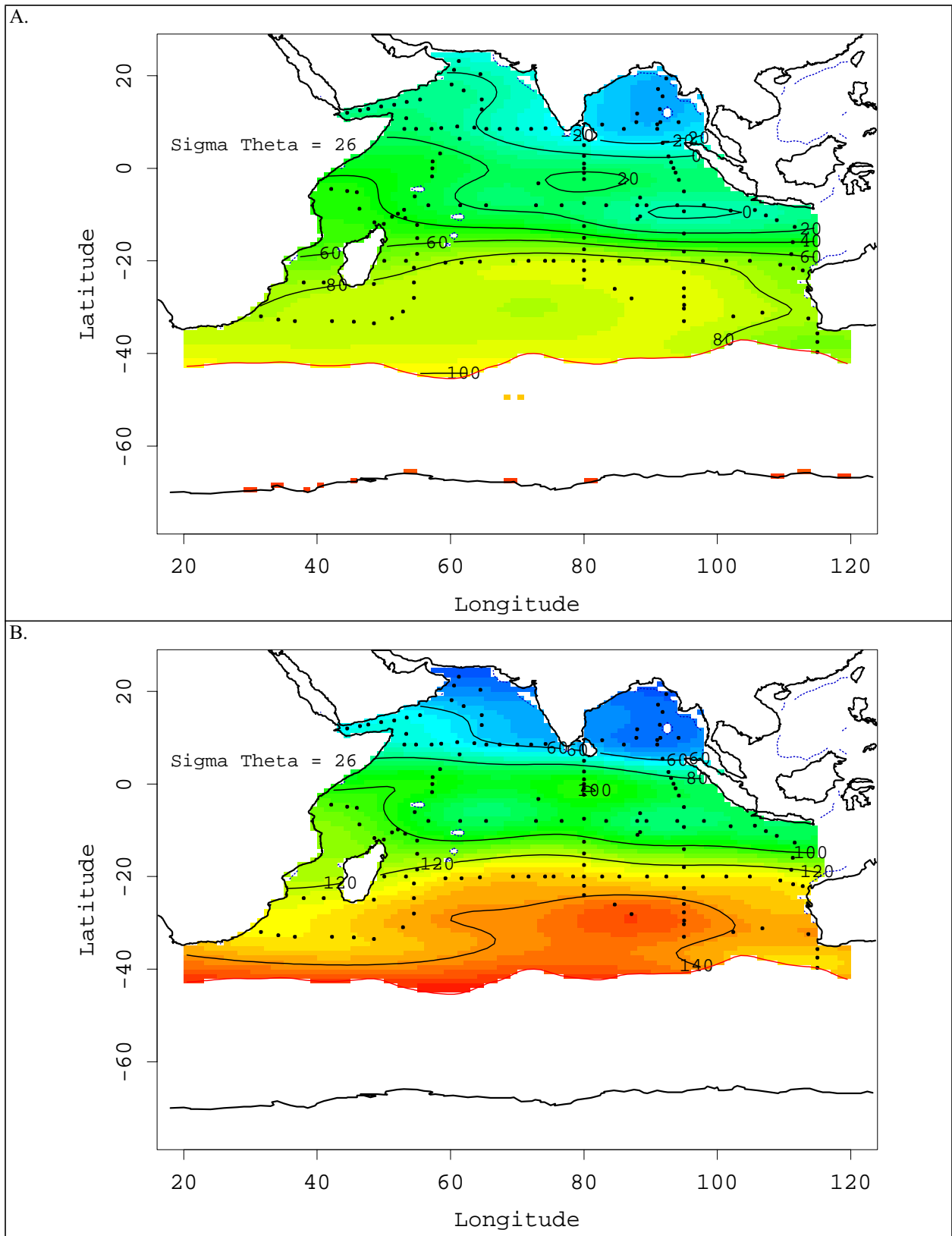


Figure 14: (A) $\Delta^{14}\text{C}$ and (B) bomb-produced $\Delta^{14}\text{C}$ on $\sigma_{\theta}=26.0$

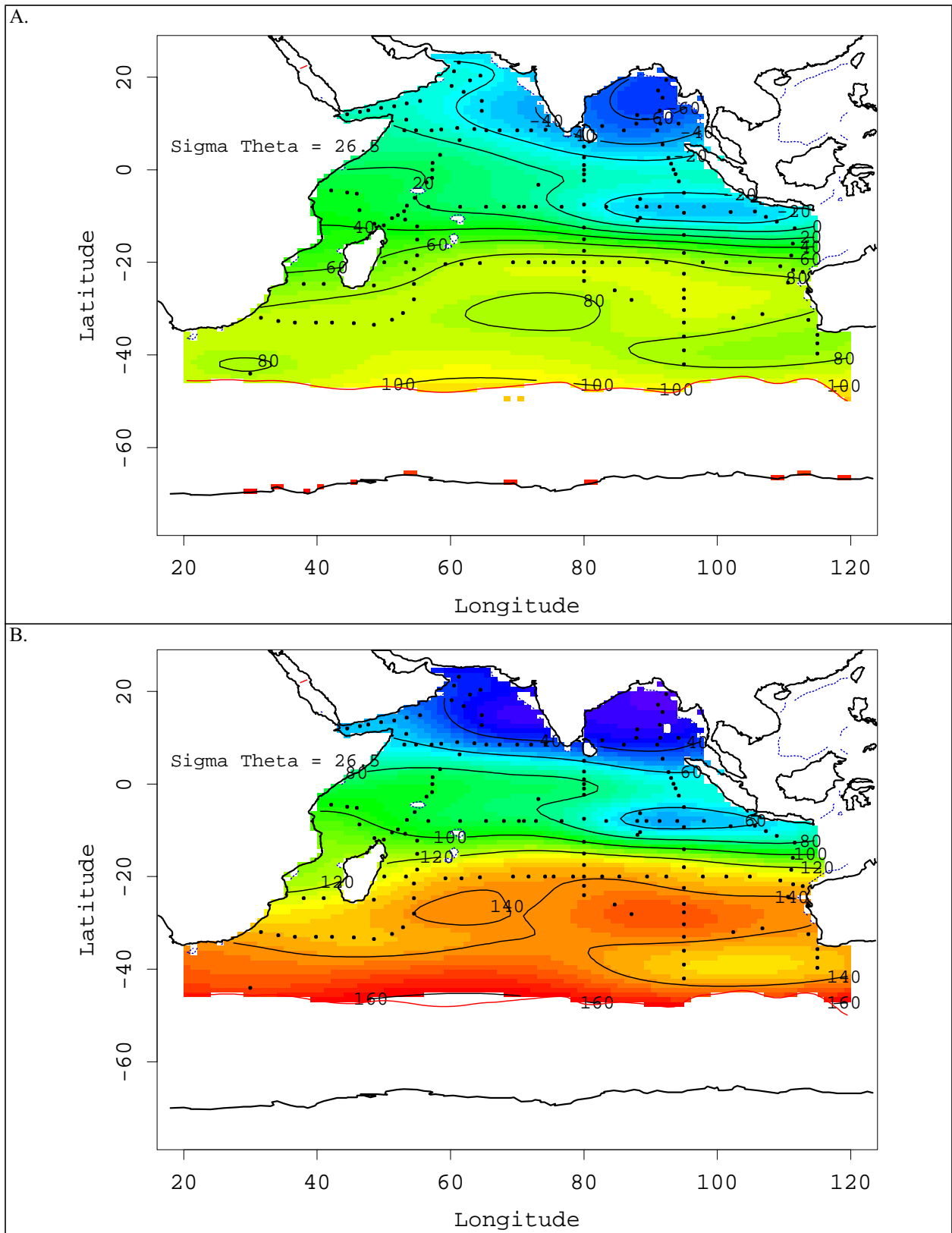


Figure 15: (A) $\Delta^{14}\text{C}$ and (B) bomb-produced $\Delta^{14}\text{C}$ on $\sigma_{\theta}=26.5$

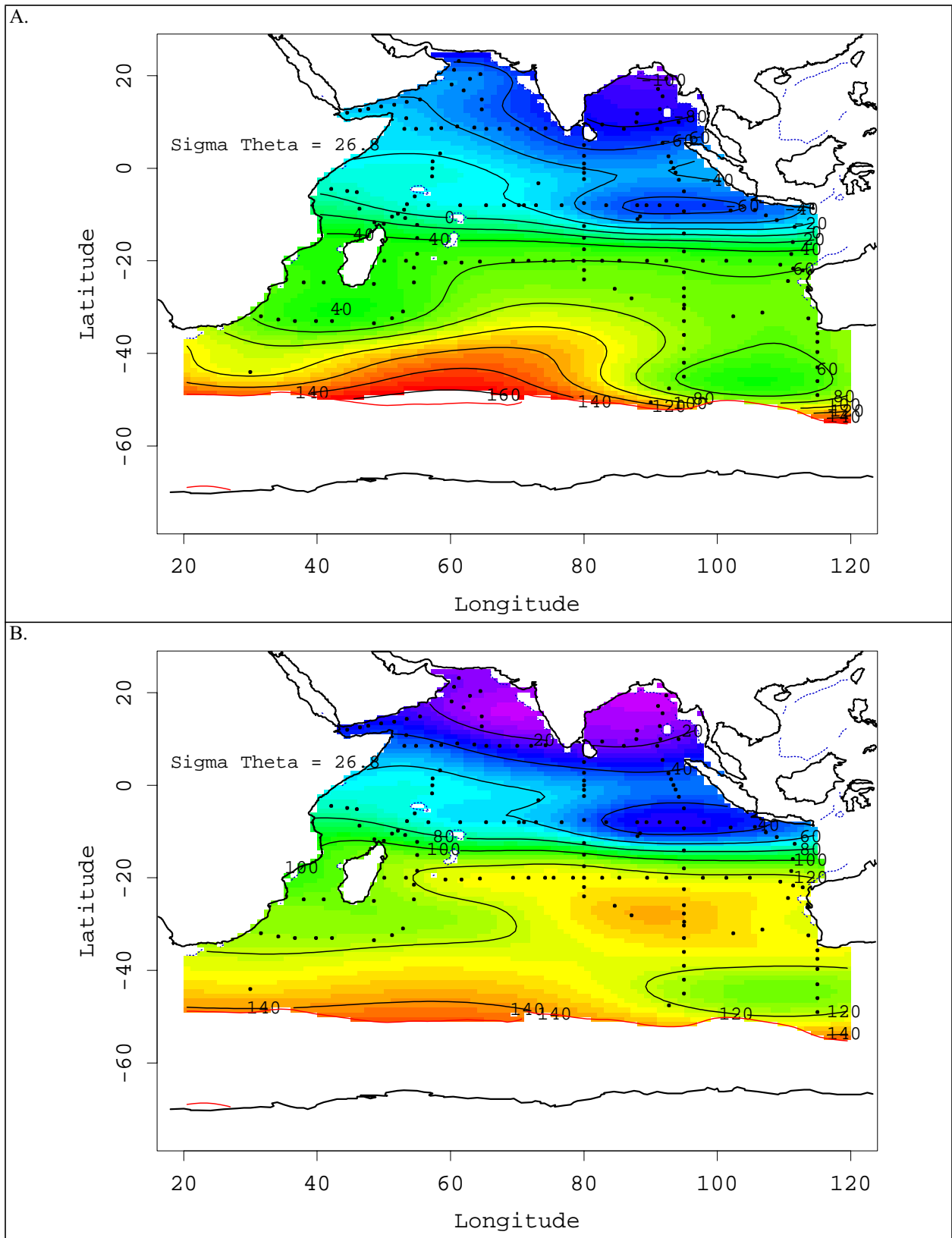


Figure 16: (A) $\Delta^{14}\text{C}$ and (B) bomb-produced $\Delta^{14}\text{C}$ on $\sigma_{\theta}=26.8$

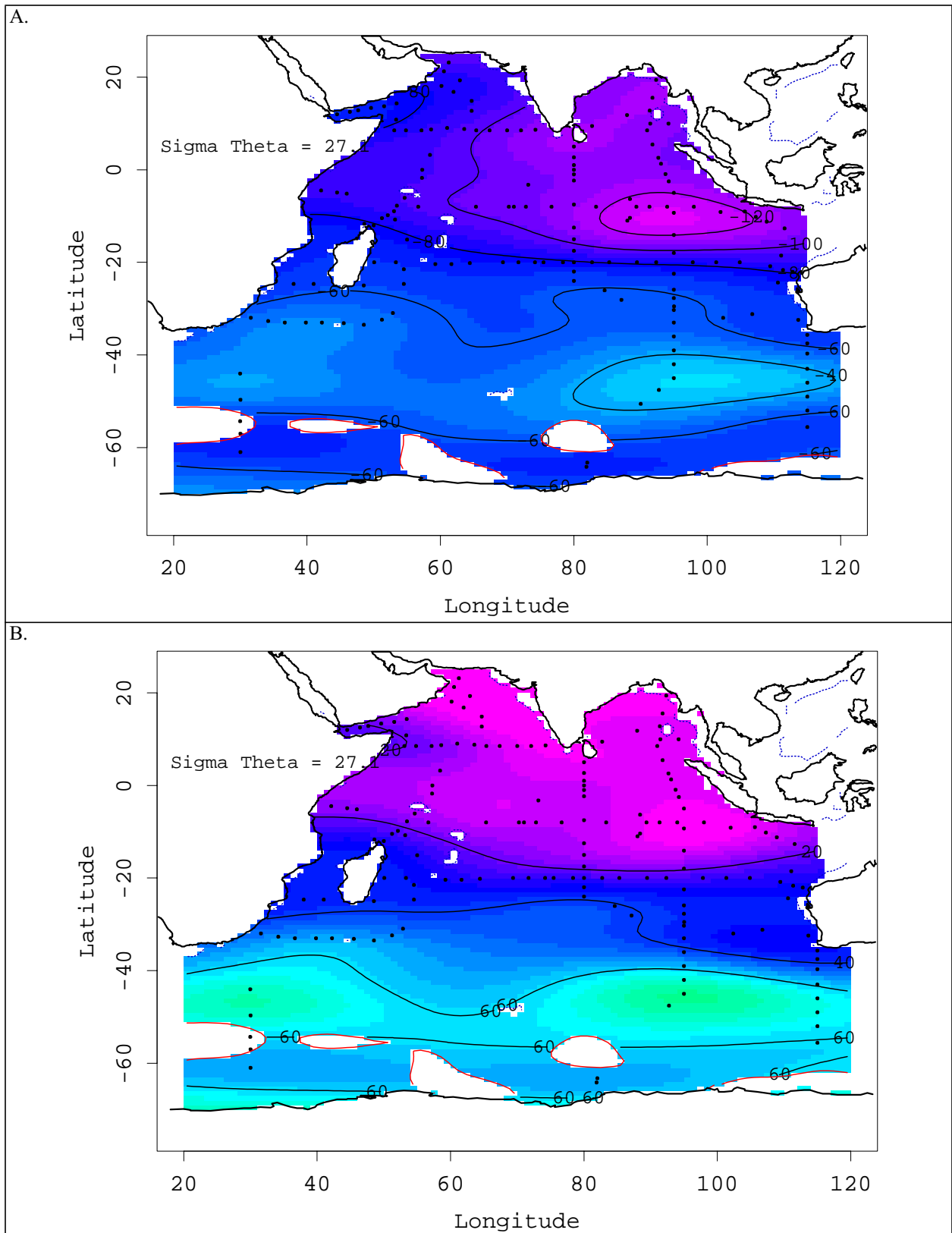


Figure 17: (A) $\Delta^{14}\text{C}$ and bomb-produced (B) $\Delta^{14}\text{C}$ on $\sigma_{\theta}=27.1$

5.0 References and Supporting Documentation

- Bard, E., M. Arnold, H.G. Ostlund, P. Maurice, P. Monfray and J.-C. Duplessy, Penetration of bomb radiocarbon in the tropical Indian Ocean measured by means of accelerator mass spectrometry, *Earth Planet. Sci. Lett.*, 87, 379-389, 1988.
- Broecker, W.S., S. Sutherland and W. Smethie, Oceanic radiocarbon: Separation of the natural and bomb components, *Global Biogeochemical Cycles*, 9(2), 263-288, 1995.
- Chambers, J.M. and Hastie, T.J., 1991, Statistical Models in S, Wadsworth & Brooks, Cole Computer Science Series, Pacific Grove, CA, 608pp.
- Chambers, J.M., Cleveland, W.S., Kleiner, B., and Tukey, P.A., 1983, Graphical Methods for Data Analysis, Wadsworth, Belmont, CA.
- Cleveland, W.S., 1979, Robust locally weighted regression and smoothing scatterplots, *J. Amer. Statistical Assoc.*, 74, 829-836.
- Cleveland, W.S. and S.J. Devlin, 1988, Locally-weighted regression: An approach to regression analysis by local fitting, *J. Am. Statist. Assoc.*, 83:596-610.
- Elder, K.L. A.P. McNichol and A.R. Gagnon, Reproducibility of seawater, inorganic and organic carbon ^{14}C results at NOSAMS, *Radiocarbon*, 40(1), 223-230, 1998
- Joyce, T., and Corry, C., eds., Corry, C., Dessier, A., Dickson, A., Joyce, T., Kenny, M., Key, R., Legler, D., Millard, R., Onken, R., Saunders, P., Stalcup, M., *contrib.*, Requirements for WOCE Hydrographic Programme Data Reporting, WHPO Pub. 90-1 Rev. 2, 145pp., 1994.
- Key, R.M., WOCE Pacific Ocean radiocarbon program, *Radiocarbon*, 38(3), 415-423, 1996.
- Key, R.M., P.D. Quay, G.A. Jones, A.P. McNichol, K.F. Von Reden and R.J. Schneider, WOCE AMS Radiocarbon I: Pacific Ocean results; P6, P16 & P17, *Radiocarbon*, 38(3), 425-518, 1996.
- Key, R.M. and P. Schlosser, S4P: Final report for AMS ^{14}C samples, Ocean Tracer Lab Technical Report 99-1, January, 1999, 11pp.
- Leboucher, V. J. Orr, P. Jean-Babtiste, M. Arnold, P. Monfrey, N. Tisnerat-Laborde, A. Poisson and J.C. Duplessey, Oceanic radiocarbon between Antarctica and South Africa along WOCE section I6 at 30°E, *Radiocarbon*, 41, 51-73, 1999.
- McNichol, A.P., G.A. Jones, D.L. Hutton, A.R. Gagnon, and R.M. Key, Rapid analysis of seawater samples at the National Ocean Sciences Accelerator Mass Spectrometry Facility, Woods Hole, MA, *Radiocarbon*, 36 (2):237-246, 1994.
- NOSAMS, National Ocean Sciences AMS Facility Data Report #99-043, Woods Hole Oceanographic Institution, Woods Hole, MA, 02543, 2/16/1999.
- Osborne, E.A. A.P. McNichol, A.R. Gagnon, D.L. Hutton and G.A. Jones, Internal and external checks in the NOSAMS sample preparation laboratory for target quality and homogeneity, *Nucl. Instr. and Methods in Phys. Res.*, B92, 158-161, 1994.

- Rubin, S. and R.M. Key, Separating natural and bomb-produced radiocarbon in the ocean: The potential alkalinity method, *Global Biogeochem. Cycles*, *in press*, 2002.
- Sabine, C.L. and R.M. Key, Surface Water and Atmospheric Underway Carbon Data Obtained During the World Ocean Circulation Experiment Indian Ocean Survey Cruises (R/V Knorr, December 1994-January 1996), ORNL/CDIAC-103, NDP-064, Carbon Dioxide Information Analysis Center, Oak Ridge National Laboratory, Oak Ridge TN, 89 pp., 1997.
- Sabine, C.L., R. Wanninkhof, R.M. Key, C. Goyet, R. Millero, Seasonal CO₂ fluxes in the tropical Indian Ocean, *Mar. Chem.*, *72*, 33-53, 2000.
- Schneider, R.J. A.P. McNichol, M.J. Nadeau and K.F. von Reden, Measurements of the oxalic acid I/oxalic acid II ratio as a quality control parameter at NOSAMS, *In Proceedings of the 15th International ¹⁴C Conference*, *Radiocarbon*, *37(2)*, 693-696, 1995.
- Stuiver, M. and H.G. Ostlund, GEOSECS Indian Ocean and Mediterranean radiocarbon, *Radiocarbon*, *25(1)*, 1-29, 1983.